

# Activation of Chlorosilanes at Ruthenium: A Route to Silyl $\sigma$ -Dihydrogen Complexes

Sébastien Lachaize, Ana Caballero, Laure Vendier, and Sylviane Sabo-Etienne\*

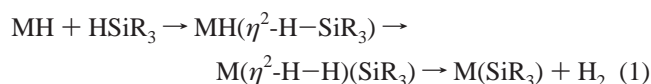
Laboratoire de Chimie de Coordination du CNRS, 205 route de Narbonne,  
31077 Toulouse Cedex 04, France

Received March 27, 2007

The hydrido  $\sigma$ -dihydrogen complex  $\text{RuClH}(\eta^2\text{-H}_2)(\text{PCy}_3)_2$  (**2**) reacts with the chlorosilanes  $\text{HSiMe}_{3-n}\text{Cl}_n$  ( $n = 1-3$ ) to form the corresponding silyl  $\sigma$ -dihydrogen complexes  $\text{RuCl}(\text{SiMe}_{3-n}\text{Cl}_n)(\eta^2\text{-H}_2)(\text{PCy}_3)_2$  (**3Me<sub>3-n</sub>Cl<sub>n</sub>**). These complexes display a 16-electron configuration, as shown by NMR, by X-ray data in the case of **3MeCl<sub>2</sub>**, and by theoretical calculations. The  $\sigma\text{-H}_2$  ligand in **3MeCl<sub>2</sub>** has been located by X-ray diffraction, and the H–H distance of 1.05(3) Å compares well with the value obtained by DFT/B3PW91 (1.073 Å) as well as with the value of  $1.08 \pm 0.01$  Å derived from the measurement of the  $J_{\text{HD}}$  coupling constant of 17.5 Hz for the deuterated isotopomer  $\text{RuCl}(\text{SiMeCl}_2)(\eta^2\text{-HD})(\text{PCy}_3)_2$ . The series of model complexes  $\text{RuCl}(\text{SiMe}_{3-n}\text{Cl}_n)(\eta^2\text{-H}_2)(\text{PMe}_3)_2$  (**S3Me<sub>3-n</sub>Cl<sub>n</sub>**) was investigated by DFT at the B3PW91 level. The most stable isomers have a structure that resembles the X-ray structure of **3MeCl<sub>2</sub>**: i.e., a silyl  $\sigma$ -dihydrogen formulation. In the case of **S3Me<sub>2</sub>Cl** and **S3MeCl<sub>2</sub>** a second minimum very close in energy was optimized and formulated as a hydrido  $\sigma$ -silane species. The influence of the number of Cl substituents on Si and their location have been analyzed. The difference between **3Me<sub>2</sub>Cl** on one side and **3MeCl<sub>2</sub>** and **3Cl<sub>3</sub>** on the other side is highlighted both by NMR and DFT data and by their reactivity toward ethylene. No reaction was observed for the latter complexes, whereas reaction with **3Me<sub>2</sub>Cl** produces the hydrido  $\eta^2$ -ethylene complex  $\text{RuClH}(\text{C}_2\text{H}_4)(\text{PCy}_3)_2$  (**4**). In the case of styrene, the arene complex  $\text{RuCl}(\text{SiMe}_2\text{Cl})(\eta^6\text{-C}_8\text{H}_{10})(\text{PCy}_3)$  (**5**) was isolated.

## Introduction

Oxidative addition of a Si–H bond to a metal center has long been considered as the pathway of choice in silane activation by transition-metal complexes.<sup>1</sup> The formation of the corresponding hydrido silyl complex represents a key step in hydrosilylation, a process with wide industrial applications.<sup>2,3</sup> However, the formation of a  $\sigma$ -silane complex as an intermediate of this elementary step is very often invoked.<sup>4</sup> Perutz and Sabo-Etienne have recently published a review on a mechanism highlighting the role of  $\sigma\text{-H-E}$  complexes (E = H, C, B, Si) in the functionalization of various substrates.<sup>5</sup> This process, called  $\sigma$ -complex assisted metathesis or  $\sigma$ -CAM, is based on the possibility of interconverting  $\sigma$ -ligands without a change in oxidation state. In the case of silane activation, addition of a silane to a metal center produces a hydrido  $\sigma$ -silane complex which can be converted to a silyl  $\sigma$ -dihydrogen complex and ultimately a silyl complex can be formed ready for subsequent functionalization (see eq 1).



As opposed to the addition–reductive elimination sequences, no change of oxidation state is required and at least two discrete

$\sigma$ -complexes are formed. It is also distinct from the well-known  $\sigma$ -bond metathesis mechanism, which involves a four-centered transition state but does not require any intermediates. In silane chemistry, the hypervalence property of silicon favors such a mechanism by allowing the formation of secondary interactions with neighboring atoms (secondary interactions between silicon and hydrogen atoms: SISHA interactions).<sup>6–8</sup> It is thus obvious that the nature of the silicon substituents will play a major role.

As part of our broad research program on silane activation by ruthenium complexes, we have considered the effect of the introduction of chlorine atom(s). Silane activation by the bis-(dihydrogen)ruthenium complex  $\text{RuH}_2(\eta^2\text{-H}_2)_2(\text{PCy}_3)_2$  (**1**) is dominated by substitution reactions of the dihydrogen ligands, leading to the corresponding silane complexes  $\text{RuH}_2(\eta^2\text{-H}_2)_{2-x}(\eta^2\text{-HSiR}_2\text{R}')_x(\text{PCy}_3)_2$  ( $x = 1, 2$ ; R, R' = alkyl, alkoxy, aryl) with one or two  $\sigma$ -silane ligands.<sup>7,9,10</sup> We have recently reported some preliminary studies concerning the catalytic activation of dimethylchlorosilane.<sup>11</sup> Stoichiometric experiments showed that, in addition to the expected mono- and disubstitution products  $\text{RuH}_2(\eta^2\text{-H}_2)(\eta^2\text{-HSiMe}_2\text{Cl})(\text{PCy}_3)_2$  and  $\text{RuH}_2(\eta^2\text{-HSiMe}_2\text{Cl})_2(\text{PCy}_3)_2$ , a third complex,  $\text{RuCl}(\text{SiMe}_2\text{Cl})(\eta^2\text{-H}_2)(\text{PCy}_3)_2$  (**3Me<sub>2</sub>Cl**),

(6) Atheaux, I.; Delpéch, F.; Donnadiéu, B.; Sabo-Etienne, S.; Chaudret, B.; Hussein, K.; Barthelat, J. C.; Braun, T.; Duckett, S. B.; Perutz, R. N. *Organometallics* **2002**, *21*, 5347–5357.

(7) Lachaize, S.; Sabo-Etienne, S. *Eur. J. Inorg. Chem.* **2006**, 2115–2127, *ibid* 4697–4699.

(8) Lin, Z. *Chem. Soc. Rev.* **2002**, *31*, 239–245.

(9) Delpéch, F.; Sabo-Etienne, S.; Daran, J. C.; Chaudret, B.; Hussein, K.; Marsden, C. J.; Barthelat, J. C. *J. Am. Chem. Soc.* **1999**, *121*, 6668–6682.

(10) Hussein, K.; Marsden, C. J.; Barthelat, J. C.; Rodriguez, V.; Conejero, S.; Sabo-Etienne, S.; Donnadiéu, B.; Chaudret, B. *Chem. Commun.* **1999**, 1315–1316.

(11) Lachaize, S.; Sabo-Etienne, S.; Donnadiéu, B.; Chaudret, B. *Chem. Commun.* **2003**, 214–215.

\* To whom correspondence should be addressed. Tel: +33 5 61 33 31 77. Fax: +33 5 61 55 30 03. E-mail: sylviane.sabo@lcc-toulouse.fr.

(1) Corey, J. Y.; Braddock-Wilking, J. *Chem. Rev.* **1999**, *99*, 175–292.

(2) Marciniak, B. *Coord. Chem. Rev.* **2005**, *249*, 2374–2390.

(3) Marciniak, B. In *Applied Homogeneous Catalysis with Organometallic Compounds*, 2nd ed.; Cornils, B., Herrmann, W. A., Eds.; Wiley: New York, 2002; p 491.

(4) Kubas, G. J. *Catal. Lett.* **2005**, *104*, 79–101.

(5) Perutz, R. N.; Sabo-Etienne, S. *Angew. Chem., Int. Ed.* **2007**, *46*, 2578–2592.

**Scheme 1.** Formation of  $\text{RuCl}(\text{SiMe}_{3-n}\text{Cl}_n)(\eta^2\text{-H}_2)(\text{PCy}_3)_2$  ( $3\text{Me}_{3-n}\text{Cl}_n$ ,  $n = 1-3$ )

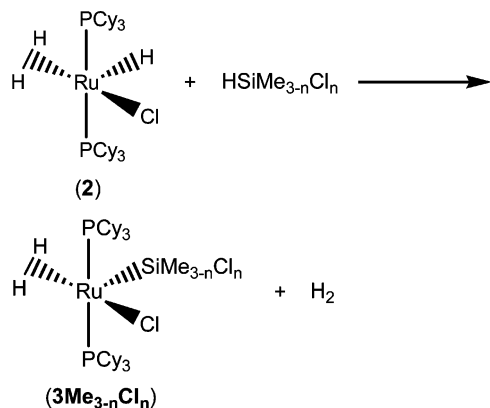


**Table 1.** NMR Data (C<sub>7</sub>D<sub>8</sub>) for Compounds  $3\text{Me}_{3-n}\text{Cl}_n$  ( $n = 1-3$ )

	$3\text{Me}_2\text{Cl}$	$3\text{MeCl}_2$	$3\text{Cl}_3$
$\delta(\sigma\text{-H}_2)$	-13.75	-12.14	-12.02
$T_1(\text{min})^a$ (253 K, 300 MHz), ms	29		23
$T_1(\text{min})^a$ (263 K, 400 MHz), ms		27	
$\delta(\text{PCy}_3)$	46.7	45.5	46.0
$\delta(\text{SiMe}_{3-n}\text{Cl}_n)$	85.7	72.6	14.8

<sup>a</sup>  $T_1(\text{min})$  values are given with an error range of 1 ms.

resulting from Si–Cl bond breaking, was detected.  $3\text{Me}_2\text{Cl}$  could be better isolated by reacting  $\text{HSiMe}_2\text{Cl}$  with the known chloro complex<sup>12</sup>  $\text{RuClH}(\eta^2\text{-H}_2)(\text{PCy}_3)_2$  (**2**). Herein we describe the reactivity of **2** with the series of chlorosilanes  $\text{HSiMe}_{3-n}\text{Cl}_n$  ( $n = 1-3$ ) leading to the isolation of a family of silyl  $\sigma$ -dihydrogen complexes  $\text{RuCl}(\text{SiMe}_{3-n}\text{Cl}_n)(\eta^2\text{-H}_2)(\text{PCy}_3)_2$  ( $3\text{Me}_{3-n}\text{Cl}_n$ ). NMR, X-ray, and DFT data are analyzed to evaluate how the number of chlorine atoms influences the silane activation and dihydrogen coordination.

## Results

**Silyl  $\sigma$ -Dihydrogen Complexes.** Complex **2** easily reacts in THF with the chlorosilanes  $\text{HSiMe}_{3-n}\text{Cl}_n$  ( $n = 1-3$ ) to form the corresponding silyl  $\sigma$ -dihydrogen complexes  $\text{RuCl}(\text{SiMe}_{3-n}\text{Cl}_n)(\eta^2\text{-H}_2)(\text{PCy}_3)_2$  ( $3\text{Me}_{3-n}\text{Cl}_n$ ) (see Scheme 1). Dihydrogen is released, according to the observed gas evolution and to the signal detected at 4.6 ppm in the in situ <sup>1</sup>H NMR spectra. These species slowly decompose in presence of an excess of chlorosilane. However, dilute NMR toluene-*d*<sub>8</sub> solutions of **3** are stable over a few days. Relevant NMR data concerning this series of complexes are given in Table 1. In the case of  $3\text{MeCl}_2$ , the  $\sigma\text{-H}_2$  ligand resonates as a broad peak at  $\delta -12.14$  in the <sup>1</sup>H NMR spectrum. The peak remained broad in the range 298–193 K. The  $T_1(\text{min})$  value of 27 ms at 253 K (400 MHz) confirms a  $\sigma$ -dihydrogen formulation (see below for more details). The <sup>31</sup>P{<sup>1</sup>H} spectrum consists of a single resonance at  $\delta 45.5$  corresponding to the equivalent phosphanes. The <sup>29</sup>Si{<sup>1</sup>H,<sup>31</sup>P} spectrum reveals a signal at  $\delta 72.6$ , in the classical range for silyl complexes.<sup>1,7</sup> Complexes  $3\text{Me}_2\text{Cl}$  and  $3\text{Cl}_3$  exhibit similar NMR data. All of these NMR data and the observation of H<sub>2</sub> evolution are consistent with the formulation of  $3\text{Me}_{3-n}\text{Cl}_n$  as 16-electron silyl  $\sigma$ -dihydrogen complexes.

We were able to determine the structure of  $3\text{MeCl}_2$  by X-ray diffraction of a single crystal at 100 K (see Figure 1). The ruthenium center is in a pseudo-octahedral environment, with

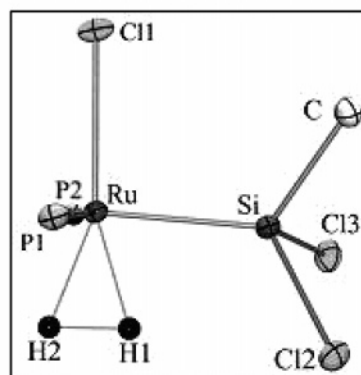
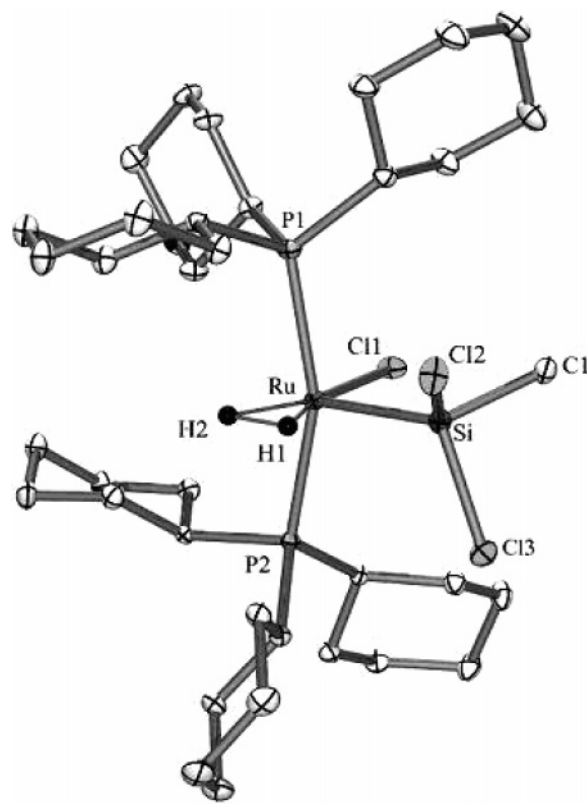


**Figure 1.** X-ray structure of  $3\text{MeCl}_2$  with a projection view along the P1–Ru–P2 axis (50% probability ellipsoids). Protons of methyl and cyclohexyl groups are omitted for clarity. Distances (Å) and angles (deg): Ru–P1 = 2.3919(5), Ru–P2 = 2.3822(5), Ru–Cl1 = 2.3819(4), Ru–Si = 2.2727(5), Ru–H1 = 1.59(2), Ru–H2 = 1.62(2), H1–H2 = 1.05(3), Si···H1 = 2.25(2), Si–Cl1 = 1.864(2), Si–Cl3 = 2.1100(7), Si–Cl2 = 2.1140(7); P1–Ru–P2 = 160.31(2), Cl1–Ru–H1 = 163.6(8), Cl1–Ru–H2 = 158.3(8), Cl1–Ru–Si = 94.85(2), H1–Ru–H2 = 38.1(8), H1–Ru–Si = 68.8(7), Cl1–Si–H1 = 153.2(8).

a vacant site trans to the  $\text{SiMeCl}_2$  group. Such an arrangement is in agreement with the trans effect of the silyl.<sup>13</sup> The Ru–Si bond length of 2.2727(5) Å is in the classical range for silyl ligands.<sup>17</sup> The phosphanes are almost trans to each other with a P1–Ru–P2 angle of 160.31(2)°. The Ru–Cl1 distance of 2.3819(4) Å is unchanged compared to that in **2** (2.380(2) Å).<sup>14</sup> The quality of the data allowed the location of the  $\sigma$ -dihydrogen ligand, although it still has to be discussed cautiously. The H1–H2 distance of 1.05(3) Å reveals a slightly elongated dihydrogen ligand located in the equatorial plane, trans to the chlorine

(12) Christ, M. L.; Sabo-Etienne, S.; Chaudret, B. *Organometallics* **1994**, *13*, 3800–3804.

(13) Zhu, J.; Lin, Z.; Marder, T. B. *Inorg. Chem.* **2005**, *44*, 9384–9390.  
(14) Lachaize, S. Thesis, Université Toulouse III-Paul Sabatier, Toulouse, France, 2004.

**Table 2. Selected Bond Distances and Angles for the DFT/B3PW91 Optimized Geometries of  $\text{RuCl}(\text{SiMe}_{3-n}\text{Cl}_n)(\eta^2\text{-H}_2)(\text{PMe}_3)_2$  ( $\text{S3Me}_{3-n}\text{Cl}_n$ ,  $n = 1-3$ ) and  $\text{RuHCl}(\eta^2\text{-H}_2)(\text{PMe}_3)_2$  ( $\text{S2}$ )<sup>a</sup>**

	$\text{S3Me}_2\text{Cl}$		$\text{S3MeCl}_2$		$\text{S2}$ (Si ≡ H <sub>3</sub> )	
	R <sub>1</sub> = Me	R <sub>1</sub> = Cl	R <sub>1</sub> = Me	R <sub>1</sub> = Cl	$\text{S3Cl}_3$	
Ru–Cl <sub>1</sub>	2.409	2.412	2.392	2.398	2.378	2.411
Cl <sub>1</sub> –R <sub>1</sub>	3.758	4.095	3.664	4.148	3.823	
Ru–P <sub>1</sub>	2.345	2.355	2.360	2.368	2.368	2.334
Ru–P <sub>2</sub>	2.356	2.355	2.359	2.359	2.368	2.334
Ru–H <sub>1</sub>	1.600	1.625	1.623	1.620	1.633	1.592
Ru–H <sub>2</sub>	1.575	1.558	1.617	1.558	1.616	1.592
Si–R <sub>1</sub>	1.893	2.145	1.881	2.120	2.090	
Si–R <sub>2</sub>	1.891 (Me)	1.888	2.129	2.124 (Cl)	2.110	
Si–R <sub>3</sub>	2.147 (Cl)	1.889	2.129	1.879 (Me)	2.110	
Si–Cl <sub>1</sub>	3.903	4.365	3.673	4.268	3.790	3.233
Ru–Si	2.318	2.320	2.286	2.291	2.270	1.555
Si–H <sub>1</sub>	2.009	1.878	2.204	1.897	2.172	1.609
H <sub>1</sub> –H <sub>2</sub>	1.387	1.659	1.073	1.561	1.063	1.221
H <sub>1</sub> –Ru–H <sub>2</sub>	51.8	62.8	38.7	58.8	38.2	45.1
H <sub>1</sub> –Ru–Si	58.3	53.4	66.1	54.8	65.3	61.5
R <sub>1</sub> –Si–H <sub>1</sub>	149.2	135.6	156.5	141.5	154.3	
P <sub>1</sub> –Ru–P <sub>2</sub>	165.8	164.4	167.1	166.0	167.5	176.8
Cl <sub>1</sub> –Ru–H <sub>2</sub>	138.7	109.3	151.8	115.3	147.4	146.1
Cl <sub>1</sub> –Ru–H <sub>1</sub>	169.5	172.1	169.6	174.1	174.4	168.8
Cl <sub>1</sub> –Ru–Si	111.3	134.5	103.4	131.0	109.2	107.3
H <sub>2</sub> –Ru–Si–H <sub>1</sub>	3.6	0.0	1.0	–1.5	2.0	0.4
R <sub>1</sub> –Si–Ru–H <sub>1</sub>	176.9	179.7	179.0	177.7	179.9	
$\Delta E_{\text{isom}}$	0.0	+6.6	0.0	+8.4		

<sup>a</sup> R<sub>1</sub> is the silicon substituent which is in the equatorial plane of the **S3** complexes; R<sub>2</sub> and R<sub>3</sub> are the others. Distances are given in Å, angles in deg, and relative energies in kJ mol<sup>–1</sup>. The corresponding X-ray data for **3MeCl<sub>2</sub>** are given in italics for comparison.

ligand. The crystal structure is in perfect agreement with the NMR data and confirms also a 16-electron formulation for **3MeCl<sub>2</sub>**.

In species incorporating hydride and  $\sigma$ -ligands, it is very often difficult to propose arrested well-defined structures. In such cases, DFT studies can greatly improve the understanding of the coordination modes of the various ligands.<sup>8,15,16</sup> Thus, in addition to the experimental work, we have performed a theoretical study on the new family of complexes using DFT at the B3PW91 level.  $\text{PMe}_3$  was selected to model the behavior of the  $\text{PCy}_3$  phosphanes. The main data for the  $\text{RuCl}(\text{SiMe}_{3-n}\text{Cl}_n)(\eta^2\text{-H}_2)(\text{PMe}_3)_2$  (**S3Me<sub>3-n</sub>Cl<sub>n</sub>**) series ( $n = 1-3$ ) are depicted in Table 2 (see also Figure 2). For comparative purpose, a DFT study was also performed on the model  $\text{RuClH}(\eta^2\text{-H}_2)(\text{PMe}_3)_2$

(15) Maseras, F.; Lledos, A.; Clot, E.; Eisenstein, O. *Chem. Rev.* **2000**, *100*, 601–636.

(16) Bader, R. F. W.; Matta, C. F.; Cortés-Guzmán, F. *Organometallics* **2004**, *23*, 6253–6263.

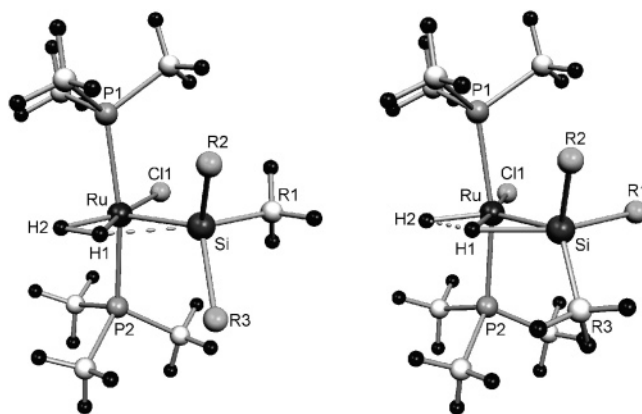


**Figure 2.** Optimized geometries of **S3MeCl<sub>2</sub>** isomers.

(**S2**). Extended Hückel calculations carried out on the related analogous iodo complex was previously reported by Eisenstein et al.<sup>17</sup> Two local minima were found on the potential energy surface for both **S3Me<sub>2</sub>Cl** and **S3MeCl<sub>2</sub>**. Their structures differ from the nature of the  $\sigma$ -ligand, either a  $\sigma$ -dihydrogen or a  $\sigma$ -silane formulation. These isomers depend on the silyl group rotation imposing either a methyl or a chloro group in the equatorial plane (this group will be referred to as R<sub>1</sub>). No geometry with a  $\sigma$ -ligand orthogonal to the equatorial plane has converged. The energies and relative stabilities of the various isomers will be discussed later. The calculated geometry of **S3MeCl<sub>2</sub>** (R<sub>1</sub> = Me) matches quite well the X-ray crystal structure of **3MeCl<sub>2</sub>**. The Ru–Si distance is 2.286 Å by DFT studies, compared to 2.2727(5) Å by X-ray studies, and the  $\sigma$ -dihydrogen bond length is 1.073 Å, compared to 1.05(3) Å. The formulation as a silyl  $\sigma$ -dihydrogen complex is thus well reproduced by the calculations. Moreover, a SISHA interaction is detected by both DFT and X-ray with comparable Si···H distances of 2.204 and 2.25(2) Å, respectively. Such an interaction could be the result of an overlap with the  $\sigma^*$  Si–C orbital of the methyl substituent. Similarly, an interaction between CO and SiR<sub>3</sub> has been evidenced by Roper et al. in the series  $\text{OsCl}(\text{SiR}_3)(\text{CO})(\text{PPh}_3)_2$ .<sup>18</sup> The rotamer of **S3MeCl<sub>2</sub>** with R<sub>1</sub> = Cl is a  $\sigma$ -silane complex with an elongated Si–H bond of 1.897 Å. The H<sub>1</sub>···H<sub>2</sub> distance (1.561 Å) is now higher than what can be found for a very stretched dihydrogen complex (limit ca. 1.4 Å).<sup>19–21</sup> The switch between the silyl  $\sigma$ -dihydrogen and the hydrido  $\sigma$ -silane isomers is also evidenced by the variation of the Cl<sub>1</sub>–Ru–H<sub>2</sub> and Cl<sub>1</sub>–Ru–Si angles. These angles are always above 100° as a result of chloride  $\pi$ -donation to the ruthenium.<sup>22</sup> The Ru–Si distance is only elongated by +0.005 Å in the  $\sigma$ -silane isomer compared to the silyl species. In the case of **S3Me<sub>2</sub>Cl** and **S3MeCl<sub>2</sub>** the existence of two rotamers, resulting from the nature of the R<sub>1</sub> ligand, leads to the optimization of  $\sigma$ -dihydrogen and  $\sigma$ -silane species. As a result of the three identical substituents (Cl) on **S3Cl<sub>3</sub>**, only one isomer was optimized in that case. It displays a  $\sigma$ -dihydrogen structure with a H<sub>1</sub>–H<sub>2</sub> bond distance of 1.063 Å. Again, a SISHA interaction is evidenced with a Si···H distance of 2.172 Å.

(17) Chaudret, B.; Chung, G.; Eisenstein, O.; Jackson, S. A.; Lahoz, F. J.; Lopez, J. A. *J. Am. Chem. Soc.* **1991**, *113*, 2314–2316.

(18) Hübler, K.; Hunt, P. A.; Maddock, S. M.; Rickard, C. E. F.; Roper, W. R.; Salter, D. M.; Schwerdtfeger, P.; Wright, L. *J. Organometallics* **1997**, *16*, 5076–5083.

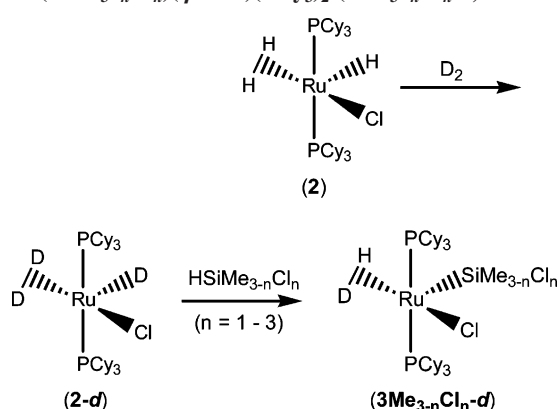
(19) Heinekey, D. M.; Lledos, A.; Lluich, J. M. *Chem. Soc. Rev.* **2004**, *33*, 175–182.

(20) Kubas, G. J. *Metal Dihydrogen and  $\sigma$ -Bond Complexes*; Kluwer Academic/Plenum Publishers: New York, 2001.

(21) Crabtree, R. H. *Angew. Chem., Int. Ed. Engl.* **1993**, *32*, 789–805.

(22) Gerard, H.; Eisenstein, O. *Dalton Trans.* **2003**, 839–845.

**Scheme 2. Synthetic Route to  $\text{RuCl}(\text{SiMe}_{3-n}\text{Cl}_n)(\eta^2\text{-HD})(\text{PCy}_3)_2$  ( $3\text{Me}_{3-n}\text{Cl}_n\text{-d}$ ,  $n = 1-3$ )**

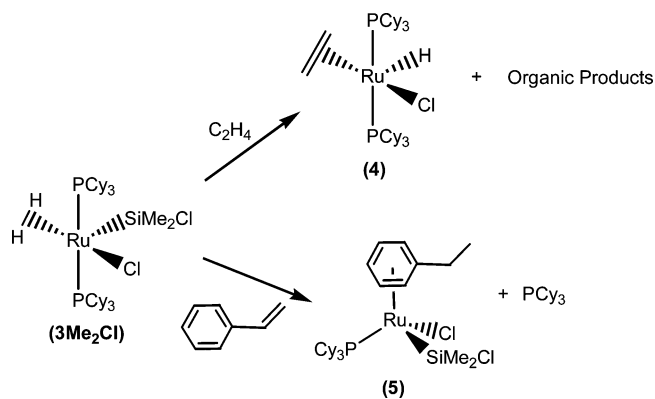


We have looked for the transition states (TS) connected to the isomerization process from the silyl  $\sigma$ -dihydrogen to the hydrido  $\sigma$ -silane species. In the case of  $3\text{Me}_2\text{Cl}$  ( $\text{R1} = \text{Me}$ ) we found a TS at  $16.0 \text{ kJ mol}^{-1}$  with a geometry resembling that of the starting material, the  $\text{SiR}_3$  group being rotated by ca.  $60^\circ$ . An increased delocalization is observed with the  $\text{H1-H2}$  distance elongated to  $1.43 \text{ \AA}$  and the  $\text{Si-H1}$  distance reduced to  $1.94 \text{ \AA}$  (the corresponding values for the minimum were  $1.38$  and  $2.09 \text{ \AA}$ ). In the case of  $3\text{MeCl}_2$  ( $\text{R1} = \text{Me}$ ) we found a TS at  $20.4 \text{ kJ mol}^{-1}$  with a geometry again resembling that of the starting complex, the  $\text{SiR}_3$  group being rotated by ca.  $60^\circ$ . In contrast, very small variations of the key parameters,  $\text{H1-H2}$  and  $\text{Si-H1}$  distances, are observed:  $1.03 \text{ \AA}$  versus  $1.07 \text{ \AA}$  for the  $\text{H1-H2}$  distance and  $2.20 \text{ \AA}$  for the  $\text{Si-H1}$  distance both in the TS and in the starting minimum. In the two systems, such a pathway allowing the isomerization of the  $\sigma$ -dihydrogen to the  $\sigma$ -silane structure has a low cost in energy. It occurs by simple rotation of the  $\text{SiR}_1\text{R}_2\text{R}_3$  group, with a fine tuning of the various interactions:  $\text{H}\cdots\text{H}$ ,  $\text{Si}\cdots\text{H}$ , and  $\text{Ru}\cdots\text{SiR}_1\text{R}_2\text{R}_3$ . An alternative pathway involving silane dissociation cannot be excluded, however, regarding the flatness of the potential energy curve and the facility of redistribution reactions at Si (see also Discussion).

**Deuteration of the Silyl  $\sigma$ -Dihydrogen Complexes.** In order to get more information on the dihydrogen ligand activation degree within this new family, we measured the  $J_{\text{HD}}$  coupling constant of the partially deuterated species  $\text{RuCl}(\text{SiMe}_{3-n}\text{Cl}_n)(\eta^2\text{-HD})(\text{PCy}_3)_2$  ( $3\text{Me}_{3-n}\text{Cl}_n\text{-d}$ ,  $n = 1-3$ ). The deuterated isomer of **2** was first prepared by exposing **2** under a  $\text{D}_2$  atmosphere. Total H/D exchange of the hydrido  $\sigma$ -dihydrogen ligands was observed within 3 min. Two equivalents of chlorosilane was then added (see Scheme 2). The hydride signal for  $3\text{Me}_{3-n}\text{Cl}_n\text{-d}$  now appears as a triplet of triplets resulting from the coupling with the two phosphorus atoms and the deuterium. No significant isotopic effect was detected at room temperature. A maximum chemical shift variation of  $\Delta\delta = -0.06 \text{ ppm}$  was measured for  $3\text{Me}_2\text{Cl}$ . The  $J_{\text{HD}}$  coupling constant values are  $12.0$ ,  $17.5$ , and  $18.9 \text{ Hz}$  for  $n = 1-3$ , respectively. Measurements of the  $J_{\text{HD}}$  values in the range  $193-293 \text{ K}$  did not lead to any significant variation.<sup>23</sup> The  $J_{\text{HD}}$  values increase with the number of chlorine substituents, meaning that the HD ligand is more elongated in  $3\text{Me}_2\text{Cl}$  than in  $3\text{MeCl}_2$  and  $3\text{Cl}_3$ . The methyl/chlorine replacement has apparently more influence on the HD activation between the two former complexes than between the two latter species.

(23) Gelabert, R.; Moreno, M.; Lluh, J. M.; Lledos, A.; Pons, V.; Heinekey, D. M. *J. Am. Chem. Soc.* **2004**, *126*, 8813–8822.

**Scheme 3. Reactivity of  $3\text{Me}_2\text{Cl}$  with Ethylene and Styrene**



**Reactivity of the Silyl  $\sigma$ -Dihydrogen Complexes.** Dihydrogen was bubbled into NMR samples of  $3\text{Me}_{3-n}\text{Cl}_n$  ( $n = 1-3$ ) in toluene- $d_8$ .  $^1\text{H}$  and  $^{31}\text{P}$  NMR monitoring showed that the starting complex immediately disappeared, leading to the formation of new species characterized by broad signals in the hydride region. Unfortunately, due to multiple exchange and redistribution processes, we were not able to isolate or characterize any species.

We have treated the silyl  $\sigma$ -dihydrogen complexes with ethylene in toluene- $d_8$ . Remarkably,  $3\text{MeCl}_2$  and  $3\text{Cl}_3$  do not react at all and are stable under an atmospheric pressure of ethylene. In contrast,  $3\text{Me}_2\text{Cl}$  gives the new hydrido  $\eta^2$ -ethylene complex  $\text{RuCl}(\text{H})(\eta^2\text{-C}_2\text{H}_4)(\text{PCy}_3)_2$  (**4**) in addition to traces of ethane, chlorodimethylvinylsilane, and chloroethyldimethylsilane (see Scheme 3). Complex **4** can be directly formed by reaction of **2** with ethylene. The  $^1\text{H}$  NMR spectrum of **4** shows a broad peak for the ethylene protons at  $\delta 2.83$  and a very shielded triplet at  $\delta -21.48$  ( $J_{\text{PH}} = 17.6 \text{ Hz}$ ), in agreement with a hydride trans to a vacant site. The 4:1 ratio for these two signals is consistent with the proposed 16-electron formulation. An analogous  $\text{P}^i\text{Pr}_3$  complex has already been experimentally and theoretically characterized.<sup>24,25</sup> The reaction is reversible, as addition of  $\text{HSiMe}_2\text{Cl}$  (2 equiv) on **4** leads to the formation of  $3\text{Me}_2\text{Cl}$  and traces of the same organic products. When  $\text{C}_2\text{H}_4$  was bubbled into a toluene- $d_8$  solution of **2** with an excess of  $\text{HSiMe}_2\text{Cl}$  (10 equiv),  $3\text{Me}_2\text{Cl}$  was the only detected complex, which means that, under these conditions, it is more stable than **4**.

Replacing ethylene by styrene yields the new silyl  $\eta^6$ -arene complex  $\text{RuCl}(\text{SiMe}_2\text{Cl})(\eta^6\text{-C}_8\text{H}_{10})(\text{PCy}_3)_2$  (**5**) (see Scheme 3). Compound **5** was fully characterized by NMR spectroscopy. Hydrogenation of styrene into ethylbenzene and coordination to the Ru center was confirmed by  $^1\text{H}$  and  $^{13}\text{C}$  NMR data. The arene resonances are shifted to higher field as a result of coordination to the metal center.<sup>26,27</sup> Five signals of equal intensity are observed between  $\delta 4.35$  and  $6.19$  in the  $^1\text{H}$  NMR spectrum, and hydrogenation of the vinyl group is evidenced by the corresponding signals of the ethyl group at  $\delta 1.06$  and  $2.29$ . The silyl ligand is characterized by two singlets at  $\delta 1.06$  and  $1.22$ , which correlate to one singlet at  $\delta 51.0$  in the  $^{29}\text{Si}\{^1\text{H}, ^{31}\text{P}\}$  NMR spectrum. Arene coordination to the metal

(24) Coalter, J. N., III; Bollinger, J. C.; Huffman, J. C.; Werner-Zwanziger, U.; Caulton, K. G.; Davidson, E. R.; Gerard, H.; Clot, E.; Eisenstein, O. *New J. Chem.* **2000**, *24*, 9–26.

(25) Gerard, H.; Clot, E.; Giessner-Prettre, C.; Caulton, K. G.; Davidson, E. R.; Eisenstein, O. *Organometallics* **2000**, *19*, 2291–2298.

(26) Burgio, J.; Yardy, N. M.; Petersen, J. L.; Lemke, F. R. *Organometallics* **2003**, *22*, 4928–4932.

(27) Borowski, A. F.; Sabo-Etienne, S.; Chaudret, B. *J. Mol. Catal. A* **2001**, *174*, 69–79.

center is the driving force of the reaction of styrene with **3Me<sub>2</sub>Cl**, leading to the formation of **5**. In situ monitoring of the addition of 1 equiv of styrene to **3Me<sub>2</sub>Cl** by <sup>1</sup>H and <sup>31</sup>P NMR showed the quantitative formation of **5** and free PCy<sub>3</sub>.

### Discussion

The reaction of the 16-electron hydrido  $\sigma$ -dihydrogen complex **2** with a series of chlorosilanes gives access to the corresponding 16-electron silyl  $\sigma$ -dihydrogen complexes **3** with concomitant dihydrogen evolution. The bonding mode of the various ligands in the coordination sphere of the metal in **3** has been evaluated by combining NMR, X-ray, and DFT studies. The bonding distance of the  $\sigma$ -dihydrogen ligand can be estimated by NMR either by  $T_1$  measurements or by deuteration experiments from the  $J_{HD}$  values.  $T_1(\text{min})$  values lead to rather large H–H distance ranges, since the physical model which is used to determine the distance is strongly dependent on the rotation speed of the  $\sigma$ -dihydrogen ligand.<sup>20,28</sup> The following ranges have been obtained: 0.99–1.24 Å for **3Me<sub>2</sub>Cl**, 0.93–1.17 Å for **3MeCl<sub>2</sub>**, and 0.95–1.19 Å for **3Cl<sub>3</sub>**. It is thus difficult to establish a trend, as the values largely overlap for the three complexes. It was possible to prepare the partially deuterated  $\sigma$ -dihydrogen complexes RuCl(SiMe<sub>3–*n*</sub>Cl<sub>*n*</sub>)( $\eta^2$ -HD)(PCy<sub>3</sub>)<sub>2</sub> (**3Me<sub>3–*n*</sub>Cl<sub>*n*</sub>-*d***, *n* = 1–3). Measurements of the  $J_{HD}$  coupling constants give access to the corresponding H–D distances by using the model developed by Gründemann et al.<sup>29</sup> The following values were obtained: 1.05 ± 0.01 Å for **3Cl<sub>3</sub>**, 1.08 ± 0.01 Å for **3MeCl<sub>2</sub>**, and 1.21 ± 0.01 Å for **3Me<sub>2</sub>Cl**. They fall within the range derived from  $T_1$  data. Introduction of only one chlorine substituent leads to the stretched dihydrogen complex **3Me<sub>2</sub>Cl**, whereas by replacing Me by one or two Cl, the complexes display a dihydrogen ligand at the unstretched/stretched borderline.<sup>19–21</sup> In the case of **3MeCl<sub>2</sub>-*d*** the  $d_{HD}$  value of 1.08 ± 0.01 Å compares well with the H–H distance of 1.05(3) Å, as determined by X-ray diffraction for **3MeCl<sub>2</sub>**. Importantly, DFT studies indicate a similar trend, with **3Me<sub>2</sub>Cl** displaying a much more stretched H–H ligand (1.387 Å) than **3MeCl<sub>2</sub>** (1.073 Å) and **3Cl<sub>3</sub>** (1.063 Å).

Various isomers were optimized at the DFT/B3PW91 level. The  $\sigma$ -dihydrogen isomer was always the lowest in energy but was almost degenerate with the  $\sigma$ -silane isomer. It should be noted that a similar situation was previously reported by Maseras and Lledos for the osmium model OsCl(CO)(PH<sub>3</sub>)<sub>2</sub>“H<sub>2</sub>SiR<sub>3</sub>”.<sup>30</sup> In our system, the strongest  $\sigma$ -donor ligand was always located trans to the empty coordination site. Thus, for the silyl  $\sigma$ -dihydrogen isomers, the silyl is trans to the vacant site, whereas for the hydrido  $\sigma$ -silane isomers, the hydride is trans to the vacant site. Moreover, in the case of **S3MeCl<sub>2</sub>** and **S3Me<sub>2</sub>Cl**, the only isomers that could be optimized with a  $\sigma$ -dihydrogen ligand had a Me in the equatorial plane. Dihydrogen isomers with a Cl in the equatorial plane never converged. No isomer with a  $\sigma$ -dihydrogen ligand orthogonal to the equatorial plane could be optimized. Notably, for both the  $\sigma$ -silane and silyl formulations, the Ru–Si distance is little affected (maximum variation of 0.006 Å). All three  $\sigma$ -dihydrogen isomers of the **S3** series present a SISHA interaction (2.009, 2.204, and 2.172 Å) between the silicon and one hydrogen of the  $\sigma$ -dihydrogen ligand. This is of course in favor of an easy process leading to a hydrido  $\sigma$ -silane isomer from the corre-

**Table 3. Thermodynamic Data (kJ mol<sup>-1</sup>) Calculated for the Reaction of RuClH( $\eta^2$ -H<sub>2</sub>)(PMe<sub>3</sub>)<sub>2</sub> (**S2**) with HSiMe<sub>3–*n*</sub>Cl<sub>*n*</sub> To Form S3Me<sub>3–*n*</sub>Cl<sub>*n*</sub> and H<sub>2</sub> (*n* = 1–3)**

	S3Me <sub>2</sub> Cl		S3MeCl <sub>2</sub>		S3Cl <sub>3</sub>
	R <sub>1</sub> = Me	R <sub>1</sub> = Cl	R <sub>1</sub> = Me	R <sub>1</sub> = Cl	
$\Delta E$	–36.9	–30.2	–63.7	–55.3	–78.3
$\Delta H^a$	–38.5	–31.0	–66.5	–56.1	–81.3
$\Delta G^a$	–14.0	–8.7	–42.1	–34.6	–62.3

<sup>a</sup> At 298.15 K.

sponding silyl  $\sigma$ -dihydrogen species. This corresponds to a prototype of the  $\sigma$ -CAM mechanism and is the microreverse pathway of the reaction illustrated in eq 1 in the Introduction.<sup>5</sup> Indeed, the two isomers of **S3MeCl<sub>2</sub>** and **S3Me<sub>2</sub>Cl** are almost degenerate: +6.6 and +8.4 kJ mol<sup>-1</sup> for the  $\sigma$ -silane, respectively. Our data complement those recently reported by Vyboishchikov and Nikonov on an iron system<sup>31</sup> and highlight again the preference of silicon to be hypervalent.

The addition of the silane compound HSiMe<sub>3–*n*</sub>Cl<sub>*n*</sub> (*n* = 1–3) to the 16-electron hydrido  $\sigma$ -dihydrogen species **2**, leading to the formation of the corresponding silyl  $\sigma$ -dihydrogen complexes **3** with concomitant dihydrogen evolution, can be analyzed by DFT by using the models **S2** and **S3**. The thermodynamic quantities are gathered in Table 3. The energy values are all negative, regardless of the number of chloro substituents on Si. We note, again, a more important difference between **S3Me<sub>2</sub>Cl** on one side and **S3MeCl<sub>2</sub>** and **S3Cl<sub>3</sub>** on the other side. We have already mentioned that when **3** was exposed to a dihydrogen atmosphere, the reactions were complex, far from just a reversible process which would give back **2** and free silane. In such a case, we would expect  $\Delta G$  values closer to 0, as was observed for example in the case of dihydrogen/dinitrogen substitution in **1**.<sup>32</sup>

Reactivity studies toward ethylene also highlight the specific properties of **3Me<sub>2</sub>Cl** versus the two other complexes. In the absence of excess silane, no reaction with ethylene was observed for **3MeCl<sub>2</sub>** and **3Cl<sub>3</sub>**, whereas addition of ethylene to **3Me<sub>2</sub>Cl** leads to the formation of the hydrido  $\eta^2$ -ethylene complex RuClH(C<sub>2</sub>H<sub>4</sub>)(PCy<sub>3</sub>)<sub>2</sub> (**4**). The reaction of **4** with 2 equiv of HSiMe<sub>2</sub>Cl leads back to **3Me<sub>2</sub>Cl**, in addition to products resulting from hydrosilylation and dehydrogenative silylation. This is in agreement with the fact that when **2** is placed under catalytic conditions, i.e., excess HSiMe<sub>2</sub>Cl and excess C<sub>2</sub>H<sub>4</sub>, we only detected **3Me<sub>2</sub>Cl** and the catalysis proceeded.

As mentioned in the Introduction, during our NMR study on dehydrogenative silylation of ethylene with chlorosilanes HSiMe<sub>3–*n*</sub>Cl<sub>*n*</sub> (*n* = 1, 2) and RuH<sub>2</sub>( $\eta^2$ -H<sub>2</sub>)<sub>2</sub>(PCy<sub>3</sub>)<sub>2</sub> (**1**) as a catalyst precursor, we detected the formation of new silane compounds as well as chloro ruthenium complexes and in particular traces of **2**.<sup>11,14</sup> The same observation was made when performing the reactions in the presence of an amine (NEt<sub>3</sub>). This excluded HCl formation in solution and confirmed that Si–Cl bond activation really occurred at the ruthenium center, leading to redistribution products.<sup>26,33,34</sup> When a large excess of HSiMe<sub>2</sub>Cl (about 20 equiv) was added to **2**, new organosilanes were detected, in agreement with redistribution reactions

(31) Vyboishchikov, S. F.; Nikonov, G. I. *Chem. Eur. J.* **2006**, *12*, 8518–8533.

(32) Ben Said, R.; Hussein, K.; Tangour, B.; Sabo-Etienne, S.; Barthelat, J. C. *J. Organomet. Chem.* **2003**, *673*, 56–66.

(33) Ben Said, R.; Hussein, K.; Barthelat, J.-C.; Atheaux, I.; Sabo-Etienne, S.; Grellier, M.; Donnadiou, B.; Chaudret, B. *Dalton Trans.* **2003**, 4139–4146.

(34) Osipov, A. L.; Gerdov, S. M.; Kuzmina, L. G.; Howard, J. A. K.; Nikonov, G. I. *Organometallics* **2005**, *24*, 587–602.

(28) Morris, R. H.; Wittebort, R. *J. Magn. Reson. Chem.* **1997**, *35*, 243–250.

(29) Gründemann, S.; Limbach, H. H.; Buntkowsky, G.; Sabo-Etienne, S.; Chaudret, B. *J. Phys. Chem. A* **1999**, *103*, 4752–4754.

(30) Maseras, F.; Lledos, A. *Organometallics* **1996**, *15*, 1218–1222.

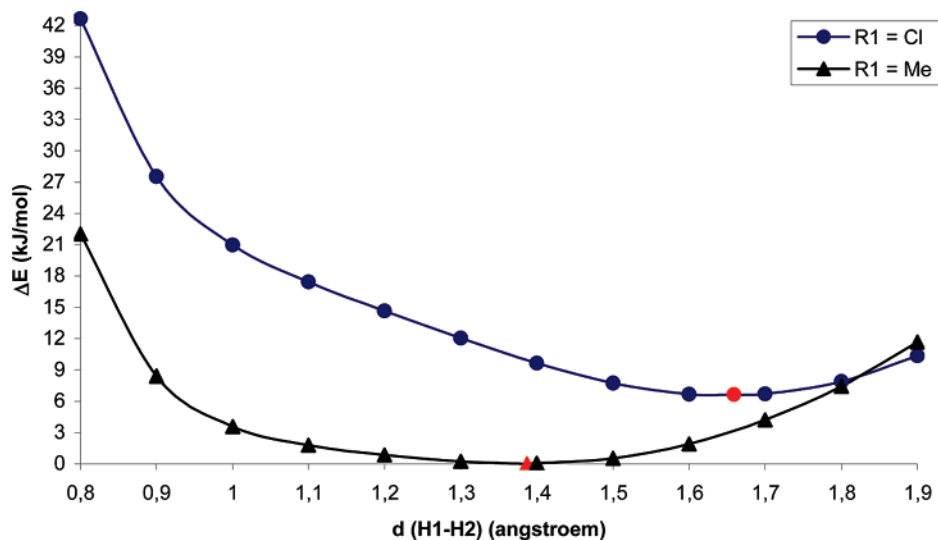


**Figure 3.** Energy profile as a function of the H1–H2 distance in **S3Me<sub>2</sub>Cl**. Comparison of the two isomers with R1 = Cl, Me.

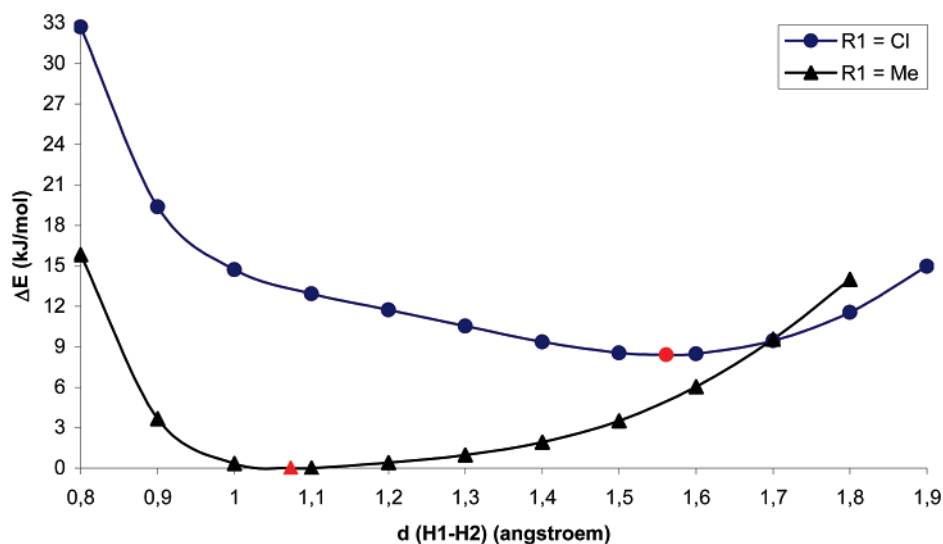


**Figure 4.** Energy profile as a function of the H1–H2 distance in **S3MeCl<sub>2</sub>**. Comparison of the two isomers with R1 = Cl, Me.

at the ruthenium center.  $\text{H}_2\text{SiMe}_2$ ,  $\text{HSiMe}_3$ , and  $\text{HSiMeCl}_2$  were in particular characterized in non-negligible quantities. Two organometallic species were identified: as expected, **3Me<sub>2</sub>Cl** was the major species, since  $\text{HSiMe}_2\text{Cl}$  was used in a very large excess, but **3MeCl<sub>2</sub>** was also detected, whereas we did not see any trace of **3Cl<sub>3</sub>**.

The difference of activity between **3Me<sub>2</sub>Cl** and the two other complexes **3MeCl<sub>2</sub>** and **3Cl<sub>3</sub>** toward ethylene can be explained by a stronger Ru–Si bond when more Cl substituents are introduced. However, it is rather surprising that, under an ethylene atmosphere, the  $\text{H}_2$  ligand remains coordinated to the Ru center. The main difference highlighted by the theoretical study is that in the case of **S3Me<sub>2</sub>Cl** (R1 = Me) the  $\sigma$ -dihydrogen ligand is extremely stretched (H–H distance of 1.387 Å) and the  $\sigma$ -silane isomer (R1 = Cl) is very close in energy (+6.6 kJ mol<sup>-1</sup>). We can assume that in **3Me<sub>2</sub>Cl** we have a delocalized system favoring ethylene coordination. In contrast, in **3MeCl<sub>2</sub>** and **3Cl<sub>3</sub>**, it is more difficult to coordinate the olefin trans to the  $\sigma$ -donor silyl ligand.

Figures 3–5 show the energy profile as a function of the H–H distance in **S3**. In the case of **S3Me<sub>2</sub>Cl** and **S3MeCl<sub>2</sub>** the two isomers resulting from the position of the substituents on Si are shown in Figures 3 and 4, respectively. The H–H distance was constrained to values varying from 0.8 to 1.9 Å, and the

optimization was conducted on all the other parameters. In the case of **S3Me<sub>2</sub>Cl** (R1 = Me) the minimum corresponds to a very stretched dihydrogen structure (H–H distance of 1.387 Å) and a very flat potential energy curve is observed from 1.0 to 1.7 Å, which means that dihydrogen activation can occur with essentially no activation barrier (Figure 3). On the other hand, for **S3Me<sub>2</sub>Cl** (R1 = Cl) the minimum corresponds to a  $\sigma$ -silane structure (Si–H1 1.878 Å) with the hydrogen H2 displaying a cis interaction with H1 (1.659 Å).<sup>15</sup> As reported by Nikonov et al., the complex  $\text{Cp}^*\text{RuCl}(\eta^2\text{-HSiMe}_2\text{Cl})(\text{PiPr}_3)$  is characterized by a  $\sigma$ -silane coordination with a stretched Ru–Si distance of 2.3982(7) Å and an additional  $\text{RuCl}\cdots\text{SiCl}$  interligand interaction.<sup>35</sup> In the case of **S3MeCl<sub>2</sub>** the minimum for (R1 = Me) now has a H–H distance of 1.073 Å and the curve is flatter for the  $\sigma$ -silane isomer (R1 = Cl) than for the  $\sigma$ -dihydrogen isomer (R1 = Me) (Figure 4). Only one isomer was optimized in the case of **S3Cl<sub>3</sub>**. It has a silyl  $\sigma$ -dihydrogen structure with a  $d_{\text{H-H}}$  distance of 1.063 Å (Si–H1 distance of 2.172 Å) (Figure 5). It is interesting here to mention that the “SiCl<sub>3</sub>” complex  $[\text{Cp}(\text{PMe}_3)_2\text{Ru}(\eta^2\text{-HSiCl}_3)]^+$  reported by Lemke et al. displays a  $\sigma$ -silane structure, as evidenced by X-ray (Si–H

(35) Osipov, A. L.; Vyboishchikov, S. F.; Dorogov, K. Y.; Kuzmina, L. G.; Howard, J. A. K.; Lemenovskii, D. A.; Nikonov, G. I. *Chem. Commun.* **2005**, 3349–3351.

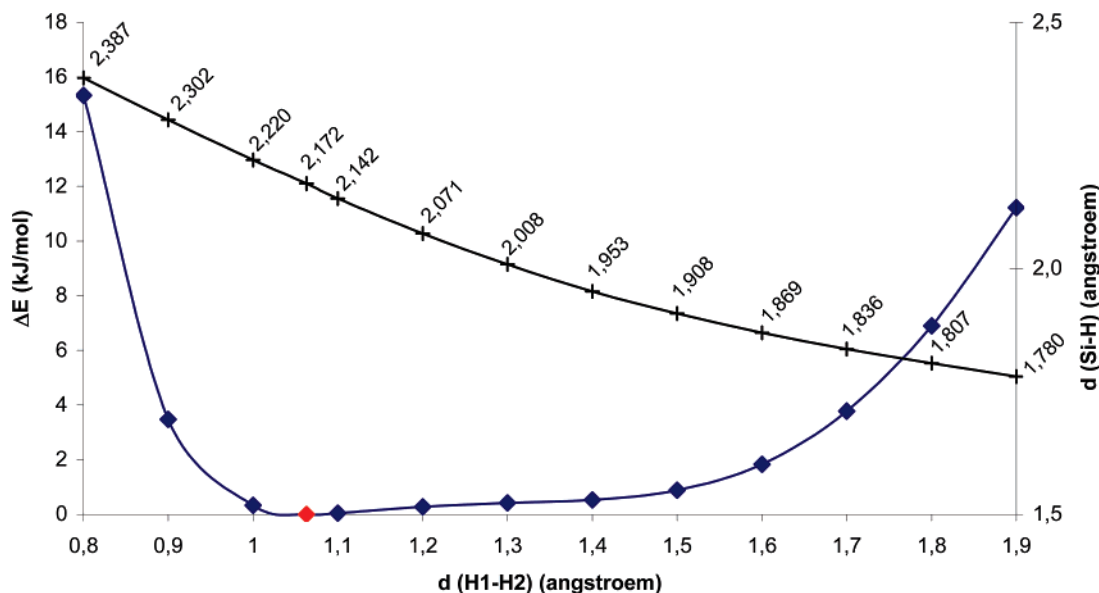


Figure 5. Energy profile and variation of the Si-H1 distance as a function of the H1-H2 distance in  $S3Cl_3$ .

Table 4. Selected Bond Distances of the Optimized Geometries of  $RuCl(SiMe_{3-n}Cl_n)(\eta^2-H_2)(PMe_3)_2$  ( $S3Me_{3-n}Cl_n$ ,  $n = 1-3$ ) with the H1-H2 Distance Constraint at 1.1 Å<sup>a</sup>

	$S3Me_2Cl$		$S3MeCl_2$		$S3Cl_3$
for SISHA consideration	$R_1 = Me$	$R_1 = Cl$	$R_1 = Me$	$R_1 = Cl$	$R_1 = Cl$
$Si \cdots H_1$	2.183	2.128	2.185	2.135	2.142
for Ru back-bonding consideration	$R_2 = Me,$ $R_3 = Cl$	$R_2 = Me,$ $R_3 = Me$	$R_2 = Cl,$ $R_3 = Cl$	$R_2 = Me,$ $R_3 = Cl$	$R_2 = Cl,$ $R_3 = Cl$
Ru-Si	2.317	2.327	2.286	2.293	2.269
$\Delta E$ (between rotamers)	0.0	+15.6	0.0	+12.9	

<sup>a</sup>  $R_1$  is the silicon substituent which is in the equatorial plane. Distances are given in Å, angles in deg, and relative energies in  $kJ mol^{-1}$ .

Table 5. Selected Bond Distances of the Optimized Geometries of  $RuCl(SiMe_{3-n}Cl_n)(\eta^2-H_2)(PMe_3)_2$  ( $S3Me_{3-n}Cl_n$ ,  $n = 1-3$ ) with the H1-H2 Distance Constraint at 1.8 Å for  $S3Me_2Cl$  and 1.7 Å for  $S3MeCl_2$ <sup>a</sup>

	$S3Me_2Cl$ (H1 $\cdots$ H2 = 1.8 Å)		$S3MeCl_2$ (H1 $\cdots$ H2 = 1.7 Å)	
for SISHA consideration	$R_1 = Me$	$R_1 = Cl$	$R_1 = Me$	$R_1 = Cl$
$Si \cdots H_1$	1.825	1.831	1.846	1.849
for Ru back-bonding consideration	$R_2 = Me,$ $R_3 = Cl$	$R_2 = Me,$ $R_3 = Me$	$R_2 = Cl,$ $R_3 = Cl$	$R_2 = Me,$ $R_3 = Cl$
Ru-Si	2.322	2.319	2.293	2.289
$\Delta E^b$	+5.6	+6.1	+9.5	+9.4

<sup>a</sup>  $R_1$  is the silicon substituent which is in the equatorial plane. Distances are given in Å, angles in deg, and relative energies in  $kJ mol^{-1}$ . <sup>b</sup> Relative to the isomer with H1 $\cdots$ H2 = 1.1 Å.

distance of 1.77(5) Å) and NMR data.<sup>36</sup> The Ru-Si distance of 2.329(1) Å is longer than that in the corresponding silyl complex  $Cp(PMe_3)_2Ru(SiCl_3)$  (2.265(2) Å). In our system, the Ru-Si distance of 2.270 Å calculated for  $S3Cl_3$  by DFT/B3PW91 is in agreement with a silyl formulation.

In order to better analyze the influence of the chloro substituents, we have reported in Tables 4 and 5 some key parameters derived from the DFT calculations. If we consider the three dihydrogen isomers  $S3Me_2Cl$ ,  $S3MeCl_2$ , and  $S3Cl_3$ , one key point on going from “ $SiMe_2Cl$ ” to “ $SiMeCl_2$ ” and finally to “ $SiCl_3$ ” is that back-donation from Ru to the  $\sigma^*$  orbital of the R2 and R3 substituents are maximized in the case of chloride versus methyl substituents. Formation of the Ru-Si

bond is thus favored. Even if the variations are rather small, this phenomenon is indicated by the shortening of the Ru-Si distances. An important study on a series of silyl complexes containing the  $CpRu(PR_3)_2$  moiety has been reported by Lemke et al. He analyzed in great detail by NMR and X-ray parameters the effect of Si substituents on the  $d(Ru)-\sigma^*(Si-R)$   $\pi$ -back-bonding interaction.<sup>37-39</sup> A similar study was performed by Nikonov et al. on the addition of  $HSiMe_{3-n}Cl_n$  ( $n = 1-3$ ) to  $Cp^*RuH_3(PR_3)$ . In that case, extensive redistribution at Si was observed, leading to a mixture of various silyl dihydride or silyl hydrido chloro complexes.<sup>34</sup> It is interesting to compare the three curves shown in Figures 3-5 and set up the  $d_{H-H}$  distance at 1.1 Å. One can see that the energy differences between the two isomers  $R_1 = Me, Cl$  for  $S3Me_2Cl$  and  $S3MeCl_2$  are similar: +15.6 and +12.9  $kJ mol^{-1}$ , respectively. The  $d_{H-H}$  distance of 1.1 Å is very close to the value found for the  $S3Cl_3$  minimum with a corresponding  $Si \cdots H$  distance of 2.142 Å, indicative of a SISHA interaction. When the  $Si \cdots H$  distances in  $S3Me_2Cl$  and  $S3MeCl_2$  are compared, it seems that SISHA are favored when  $R_1$  is a chloride. If we now consider the intercepts of the two curves shown in Figures 3 and 4, H-H distances of 1.8 and 1.7 Å are found for  $S3Me_2Cl$  and  $S3MeCl_2$ , respectively, with an energy difference with the points at 1.1 Å, of ca. 6 and 9.5  $kJ mol^{-1}$ , respectively. Again, the energy differences are small, but an increase is observed when adding more chloride,

(37) Lemke, F. R.; Galat, K. J.; Youngs, W. J. *Organometallics* **1999**, *18*, 1419-1429.

(38) Freeman, S. T. N.; Lofton, L. L.; Lemke, F. R. *Organometallics* **2002**, *21*, 4776-4784.

(39) Freeman, S. T. N.; Petersen, J. L.; Lemke, F. R. *Organometallics* **2004**, *23*, 1153-1156.

(36) Freeman, S. T. N.; Lemke, F. R.; Brammer, L. *Organometallics* **2002**, *21*, 2030-2032.

which is consistent with a more advanced Si–H activation. For the values at 1.7–1.8 Å ( $\sigma$ -silane formulation), the position of the Si substituents is not as important as it was for a value of 1.1 Å ( $\sigma$ -dihydrogen formulation).

### Conclusion

Addition of chlorosilanes to the 16-electron complex  $\text{RuClH}(\eta^2\text{-H}_2)(\text{PCy}_3)_2$  leads to dihydrogen evolution and formation of the corresponding silyl  $\sigma$ -dihydrogen complexes  $\text{RuCl}(\text{SiMe}_{3-n}\text{Cl}_n)(\eta^2\text{-H}_2)(\text{PCy}_3)_2$ . Several pathways can be proposed to achieve the final products. Coordination of the silane to the unsaturated species could lead to the 18-electron  $\sigma$ -dihydrogen  $\sigma$ -silane species  $\text{RuClH}(\eta^2\text{-HSiMe}_{3-n}\text{Cl}_n)(\eta^2\text{-H}_2)(\text{PCy}_3)_2$ . Evolution of dihydrogen, followed by oxidative addition of the silane, would result in the formation of the ruthenium(IV) dihydride complex  $\text{RuClH}_2(\text{SiMe}_{3-n}\text{Cl}_n)(\text{PCy}_3)_2$ . Then, isomerization of the dihydride into a  $\sigma$ -dihydrogen ligand would result in the final product with a ruthenium in the reduced oxidation state II. Alternatively, the first step could simply be the substitution of the  $\sigma$ -dihydrogen ligand by the silane.

In view of all the data concerning the  $\sigma$ -silane complexes, especially in ruthenium chemistry, a mechanism implying a  $\sigma$ -CAM sequence can be proposed.<sup>5</sup> Substitution of the  $\sigma$ -dihydrogen ligand by the silane results in the formation of the  $\sigma$ -silane species  $\text{RuClH}(\eta^2\text{-HSiMe}_{3-n}\text{Cl}_n)(\text{PCy}_3)_2$ . Then, a  $\sigma$ -CAM process leads to the formation of the  $\sigma$ -dihydrogen complex  $\text{RuCl}(\text{SiMe}_{3-n}\text{Cl}_n)(\eta^2\text{-H}_2)(\text{PCy}_3)_2$ . The most significant trend to note is the importance of the location of the Cl substituents which favor either a  $\sigma$ -silane or a  $\sigma$ -dihydrogen coordination. The establishment of secondary interactions (SISHA) between the silicon and the hydrogen atoms allows such a process to occur with no activation barrier. Our system illustrates perfectly a  $\sigma$ -CAM sequence as in eq 1. Moreover, as already pointed out by Lemke, the influence of the Si substituents has to be taken into account, since the effect on the electron density transferred from Ru to Si–R is greatly influenced by the nature of the R substituents.

Another alternative implying dihydrogen formation by direct reaction of the hydride with the free silane cannot be excluded, and further investigations will be performed to get more information on the mechanism of the overall process.

It is remarkable that no reaction was observed with ethylene in the case of **3MeCl<sub>2</sub>** and **3Cl<sub>3</sub>**, whereas the ethylene complex **4** was obtained in the case of **3Me<sub>2</sub>Cl**. The trans silyl effect more prominent in **3MeCl<sub>2</sub>** and **3Cl<sub>3</sub>** might prevent any coordination in the vacant site, whereas for **3Me<sub>2</sub>Cl**, the SISHA interaction between the silicon and one hydrogen of the stretched dihydrogen ligand allows the formation of **4**.

### Experimental Section

**General Methods.** All reactions were performed using standard Schlenk or drybox techniques under argon. Solvents were dried and distilled prior to use. All reagents were purchased from Aldrich, except  $\text{RuCl}_3 \cdot 3\text{H}_2\text{O}$ , which came from Johnson Matthey Ltd., and were used without further purification. NMR solvents were dried using appropriate methods and degassed prior to use. NMR samples of sensitive compounds were all prepared under an argon atmosphere, using NMR tubes fitted with Teflon septa. NMR spectra were recorded on Bruker DPX 300 (with  $^1\text{H}$  at 300.13 MHz,  $^{31}\text{P}$  at 121.49 MHz, and  $^{13}\text{C}$  at 75.46 MHz), AMX 400 (with  $^1\text{H}$  at 400.13 MHz,  $^{31}\text{P}$  at 161.98 MHz,  $^{13}\text{C}$  at 100.62 MHz,  $^{29}\text{Si}$  at 79.50 MHz, and  $^2\text{H}$  at 61.42 MHz), and AV 500 spectrometers (with  $^1\text{H}$  at 500.33 MHz,  $^{31}\text{P}$  at 202.55 MHz,  $^{13}\text{C}$  at 125.82 MHz, and  $^{29}\text{Si}$  at 99.40 MHz). Crystal data were collected at low temperature on an

Xcalibur Oxford Diffraction diffractometer, equipped with an Oxford Cryosystems cryostream cooler device and using graphite-monochromated  $\text{Mo K}\alpha$  radiation ( $\lambda = 0.71073 \text{ \AA}$ ). The complex  $\text{RuH}_2(\eta^2\text{-H}_2)_2(\text{PCy}_3)_2$  (**1**) was prepared according to published procedures.<sup>40</sup>

**RuClH( $\eta^2\text{-H}_2$ )(PCy<sub>3</sub>)<sub>2</sub> (**2**). Method a.** Addition of  $\text{HSiMe}_2\text{Cl}$  (33.2  $\mu\text{L}$ , 0.30 mmol) at 0 °C to a stirred suspension of **1** (100.0 mg, 0.15 mmol) in 4 mL of pentane resulted in gas evolution and in immediate dissolution. An orange solid precipitated after 10 min. About 30 min later, the solution was filtered off and the solid was washed with pentane (2  $\times$  1.5 mL) at 0 °C, before being dried under an argon flow and vacuum (40% yield).

**Method b.** Addition of a hexane solution of  $\text{CIBCy}_2$  (0.85 mL, 0.85 mmol) to a stirred suspension of **1** (407 mg, 0.61 mmol) in pentane (4 mL) resulted in slow dissolution and progressive orange coloration. A solid was formed after 45 min at room temperature. The solution was filtered off at –60 °C, and the solid was washed with pentane (2  $\times$  1.5 mL). The orange solid was dried under an argon flow and vacuum (95% yield).

$^1\text{H}$  NMR ( $\text{C}_6\text{D}_6$ , 293 K, 300.13 MHz):  $\delta$  –16.07 (br s, 3H,  $\text{RuH}_3$ ), 0.9–2.4 (66H,  $\text{PCy}_3$ ).  $^{31}\text{P}\{^1\text{H}\}$  NMR ( $\text{C}_6\text{D}_6$ , 293 K, 121.49 MHz):  $\delta$  53.6 (s). Anal. Calcd for  $\text{C}_{36}\text{H}_{69}\text{ClP}_2\text{Ru}$ : C, 61.72; H, 9.94. Found: C, 61.37; H, 9.88.

**RuCl(SiMe<sub>2</sub>Cl)( $\eta^2\text{-H}_2$ )(PCy<sub>3</sub>)<sub>2</sub> (**3Me<sub>2</sub>Cl**).** Addition of 25  $\mu\text{L}$  of  $\text{HSiMe}_2\text{Cl}$  (0.23 mmol) to a solution of **2** (20 mg, 0.028 mmol) in 0.5 mL of THF resulted in gas evolution, and the solution darkened. An orange solid precipitated after 12 h at –30 °C. It was filtered and dried in vacuo (79% yield).

$^1\text{H}$  NMR ( $\text{C}_7\text{D}_8$ , 288 K, 400.13 MHz):  $\delta$  –13.75 (br t,  $^2J_{\text{PH}} = 9.7 \text{ Hz}$ , 2H,  $\text{Ru}(\sigma\text{-H}_2)$ ), 1.41 (s,  $\text{SiMe}_2$ ).  $T_1(\text{min})$  ( $\text{C}_7\text{D}_8$ , 253 K, 300.13 MHz): 29 ms for the high-field signal.  $^{31}\text{P}\{^1\text{H}\}$  NMR ( $\text{C}_7\text{D}_8$ , 288 K, 161.97 MHz):  $\delta$  46.7 (s).  $^{29}\text{Si}\{^1\text{H}, ^{31}\text{P}\}$  NMR ( $\text{C}_7\text{D}_8$ , 288 K, 79.49 MHz):  $\delta$  85.7 (s). Anal. Calcd for  $\text{C}_{38}\text{H}_{74}\text{Cl}_2\text{P}_2\text{RuSi}$ : C, 57.55; H, 9.41. Found: C, 57.58; H, 8.89.

For comparison, NMR data for the free silane  $\text{HSiMe}_2\text{Cl}$  are as follows.  $^1\text{H}$  NMR ( $\text{C}_7\text{D}_8$ , 293 K, 400.13 MHz):  $\delta$  4.92 (septet,  $^1J_{\text{SiH}} = 223.3 \text{ Hz}$ , SiH).  $^{29}\text{Si}\{^1\text{H}\}$  NMR ( $\text{C}_7\text{D}_8$ , 293 K, 79.49 MHz):  $\delta$  –11.1 (s). The  $^{29}\text{Si}$  chemical shift was taken from ref 41.

**RuCl(SiMeCl<sub>2</sub>)( $\eta^2\text{-H}_2$ )(PCy<sub>3</sub>)<sub>2</sub> (**3MeCl<sub>2</sub>**).** Addition of 4.6  $\mu\text{L}$  of  $\text{HSiMeCl}_2$  (0.044 mmol) to a suspension of **2** (31.0 mg, 0.044 mmol) in 3 mL of pentane resulted in total dissolution of the solid. The resulting orange solution, kept at room temperature for 24 h, gave small dark orange crystals suitable for X-ray measurements. This compound was isolated using the same procedure as for **3Me<sub>2</sub>Cl**: addition of 25  $\mu\text{L}$  of  $\text{HSiMe}_2\text{Cl}$  (0.24 mmol) to a solution of **2** (20 mg, 0.028 mmol) in 0.5 mL of THF resulted in gas evolution, and the solution darkened. An orange solid precipitated after 12 h at –30 °C. It was filtered and dried in vacuo.

$^1\text{H}$  NMR ( $\text{C}_7\text{D}_8$ , 293 K, 400.13 MHz):  $\delta$  –12.14 (br, 2H,  $\text{Ru}(\sigma\text{-H}_2)$ ), 1.78 (s, SiMe).  $T_1(\text{min})$  ( $\text{C}_7\text{D}_8$ , 253 K, 400.13 MHz): 27 ms for the high-field signal.  $^{31}\text{P}\{^1\text{H}\}$  NMR ( $\text{C}_7\text{D}_8$ , 293 K, 161.97 MHz):  $\delta$  45.5 (s).  $^{29}\text{Si}\{^1\text{H}, ^{31}\text{P}\}$  NMR ( $\text{C}_7\text{D}_8$ , 293 K, 79.49 MHz):  $\delta$  72.6 (s). Anal. Calcd for  $\text{C}_{37}\text{H}_{71}\text{Cl}_2\text{P}_2\text{RuSi}$ : C, 54.63; H, 8.80. Found: C, 54.82; H, 8.88.

For comparison, NMR data for the free silane  $\text{HSiMeCl}_2$  are as follows.  $^1\text{H}$  NMR ( $\text{C}_7\text{D}_8$ , 293 K, 400.13 MHz):  $\delta$  5.32 (quar,  $^1J_{\text{SiH}} = 282.4 \text{ Hz}$ , SiH).  $^{29}\text{Si}\{^1\text{H}\}$  NMR ( $\text{C}_7\text{D}_8$ , 293 K, 79.49 MHz):  $\delta$  –14.7 (s).

**RuCl(SiCl<sub>3</sub>)( $\eta^2\text{-H}_2$ )(PCy<sub>3</sub>)<sub>2</sub> (**3Cl<sub>3</sub>**).** Addition of 4  $\mu\text{L}$  of  $\text{HSiCl}_3$  (0.042 mmol) to a solution of **2** (20 mg, 0.028 mmol) in 0.5 mL of THF resulted in darkening of the pale orange solution. An orange solid precipitated after 12 h at –30 °C. It was filtered and dried in vacuo.

(40) Borowski, A. F.; Sabo-Etienne, S.; Christ, M. L.; Donnadiu, B.; Chaudret, B. *Organometallics* **1996**, *15*, 1427–1434.

(41) Dubois Murphy, P.; Taki, T.; Sogabe, T.; Metzler, R.; Squires, T. G.; Gerstein, B. C. *J. Am. Chem. Soc.* **1979**, *101*, 4055–4058.



$^1\text{H}$  NMR ( $\text{C}_7\text{D}_8$ , 293 K, 300.13 MHz):  $\delta$  -12.02 (br t,  $^2J_{\text{PH}} = 9.0$  Hz, 2H, Ru( $\sigma\text{-H}_2$ )).  $T_1(\text{min})$  ( $\text{C}_7\text{D}_8$ , 253 K, 300.13 MHz): 23 ms for the high-field signal.  $^{31}\text{P}\{^1\text{H}\}$  NMR ( $\text{C}_7\text{D}_8$ , 293 K, 161.97 MHz):  $\delta$  46.0 (s).  $^{29}\text{Si}\{^1\text{H}, ^{31}\text{P}\}$  NMR ( $\text{C}_7\text{D}_8$ , 293 K, 99.40 MHz):  $\delta$  14.8 (s). Anal. Calcd for  $\text{C}_{36}\text{H}_{68}\text{Cl}_4\text{P}_2\text{RuSi}$ : C, 51.85; H, 8.22. Found: C, 52.63; H, 8.01.

For comparison, NMR data for the free silane  $\text{HSiCl}_3$  are as follows.  $^1\text{H}$  NMR ( $\text{C}_7\text{D}_8$ , 293 K, 400.13 MHz):  $\delta$  5.73 (s,  $^1J_{\text{SiH}} = 370.6$  Hz, SiH).  $^{29}\text{Si}\{^1\text{H}\}$  NMR ( $\text{C}_7\text{D}_8$ , 293 K, 79.49 MHz):  $\delta$  -9.6 (s).

**RuClH( $\eta^2\text{-C}_2\text{H}_4$ )(PCy<sub>3</sub>)<sub>2</sub> (4).** Complex **4** resulted from  $\text{C}_2\text{H}_4$  bubbling into a  $\text{C}_7\text{D}_8$  solution of **2** (13.0 mg, 0.019 mmol). NMR measurements of the sample showed the formation of **4** as the only organometallic species.  $^1\text{H}$  NMR ( $\text{C}_7\text{D}_8$ , 273 K, 400.13 MHz):  $\delta$  -21.48 (t,  $^2J_{\text{PH}} = 17.6$  Hz, 1H, RuH), 2.83 (br, 4H,  $\text{RuC}_2\text{H}_4$ ).  $^{31}\text{P}\{^1\text{H}\}$  NMR ( $\text{C}_7\text{D}_8$ , 273 K, 161.97 MHz):  $\delta$  36.5 (s).  $^{13}\text{C}\{^1\text{H}\}$  NMR ( $\text{C}_7\text{D}_8$ , 273 K, 100.62 MHz):  $\delta$  38.7 (br,  $\text{C}_2\text{H}_4$ ). Any attempt to isolate **4** failed.

**RuCl(SiMe<sub>2</sub>Cl)( $\eta^6\text{-C}_8\text{H}_{10}$ )(PCy<sub>3</sub>) (5).** Addition of 2.3  $\mu\text{L}$  of styrene (0.02 mmol) to a solution of **3Me<sub>2</sub>Cl** (15 mg, 0.02 mmol) in 1 mL of toluene resulted in an orange solution. The solution was stirred overnight, and then the volatiles were removed under reduced pressure, affording an orange oil. Stirring in pentane (2–3 mL) resulted in the formation of an orange solid at room temperature (95% yield).  $^1\text{H}$  NMR ( $\text{C}_7\text{D}_8$ , 293 K, 300.13 MHz):  $\delta$  1.06 (s, 3H, SiMe), 1.06 (t,  $^3J_{\text{HH}} = 8$  Hz, 3H,  $\text{CH}_3$  (Et)), 1.22 (s, 3H, SiMe), 1.60–1.90 (m, 33H, Cy), 2.29 (q,  $^3J_{\text{HH}} = 8$  Hz, 2H,  $\text{CH}_2$  (Et)), 4.35 (t,  $^3J_{\text{HH}} = 5.2$  Hz, 1H, aromatic), 4.49 (d,  $^3J_{\text{HH}} = 5.8$  Hz, 1H, aromatic), 4.86 (q,  $^3J_{\text{HH}} = 5.3$  Hz, 1H, aromatic), 5.39 (d,  $^3J_{\text{HH}} = 5.7$  Hz, 1H, aromatic), 6.19 (t,  $^3J_{\text{HH}} = 5.3$  Hz, 1H, aromatic).  $^{13}\text{C}\{^1\text{H}\}$  NMR ( $\text{C}_7\text{D}_8$ , 293 K, 75.46 MHz):  $\delta$  11.7, 12.2, 14.5, 25.1, 26.8, 27.8, 27.9, 30.9, 71.7, 84.0, 84.6, 93.3, 97.3, 120.2.  $^{31}\text{P}\{^1\text{H}\}$  NMR ( $\text{C}_7\text{D}_8$ , 293 K, 121.49 MHz):  $\delta$  36.7 (s).  $^{29}\text{Si}\{^1\text{H}, ^{31}\text{P}\}$  NMR ( $\text{C}_7\text{D}_8$ , 293 K, 99.40 MHz):  $\delta$  51.0 (s). Anal. Calcd for  $\text{C}_{28}\text{H}_{49}\text{Cl}_2\text{PRuSi}$ : C, 54.53; H, 8.01. Found: C, 54.01; H, 7.38.

**Computational Details.** DFT calculations were performed with the Gaussian 98 series of programs<sup>42</sup> using the nonlocal hybrid functional denoted as B3PW91.<sup>43,44</sup> For ruthenium, the core electrons were represented by a relativistic small-core pseudopo-

tential using the Durand–Barthelat method.<sup>45</sup> The 16 electrons corresponding to the 4s, 4p, 4d, and 5s atomic orbitals were described by a (7s, 6p, 6d) primitive set of Gaussian functions contracted to (5s, 5p, 3d). Standard pseudopotentials developed in Toulouse were used to describe the atomic cores of all other non-hydrogen atoms (C, Si, P, and Cl).<sup>46</sup> A double- $\zeta$  plus polarization valence basis set was employed for each atom (d-type function exponents were 0.80, 0.45, 0.45, and 0.65, respectively). For hydrogen, a standard primitive (4s) basis contracted to (2s) was used. A p-type polarization function (exponent 0.9) was added for the hydrogen atoms directly bound to ruthenium. The geometries of the various critical points on the potential energy surface were fully optimized with the gradient method available in Gaussian 98. Calculations of harmonic vibrational frequencies were performed to determine the nature of each critical point. Constraints were used only to calculate the potential energy curve along the  $\text{H1}\cdots\text{H2}$  distance axis in the S3 series of complexes. The same calculations using the B3LYP functional<sup>43,47</sup> gave similar results, but the relevant theoretical data were not as good as with B3PW91 in comparison to the experimental data (see the Supporting Information).

**Acknowledgment.** We thank the CNRS for support and the CINES (Montpellier, France) for a generous allocation of computer time. We gratefully acknowledge Prof. J.-C. Barthelat and Dr. E. Clot for fruitful discussions on the theoretical study. S.L. thanks the French Ministry “Education Nationale, Enseignement Supérieur, Recherche” for his AMN grant. A.C. thanks the Spanish “Ministerio de Educacion y Ciencia” for a post-doctoral fellowship.

**Supporting Information Available:** Text and tables giving computational details and CIF files giving crystallographic data. This material is available free of charge via the Internet at <http://pubs.acs.org>.

OM700295G

(43) Becke, A. D. *J. Chem. Phys.* **1993**, *98*, 5648–5652.

(44) Perdew, J. P.; Wang, Y. *Phys. Rev. B* **1992**, *45*, 13244–13249.

(45) Durand, P.; Barthelat, J. C. *Theor. Chim. Acta* **1975**, *38*, 283–302.

(46) Bouteiller, Y.; Mijoule, C.; Nizam, M.; Barthelat, J. C.; Daudey, J.

P.; Pelissier, M.; Silvi, B. *Mol. Phys.* **1988**, *65*, 295–312.

(47) Lee, C.; Yang, W.; Parr, R. G. *Phys. Rev. B* **1988**, *37*, 785–789.

(42) Frisch, M. J., et al. *Gaussian 98*, revision A.11; Gaussian, Inc., Pittsburgh, PA, 2001.